Cell Proliferation

Cell Prolif., 2014, **47**, 448–456 doi: 10.1111/cpr.12120

A TALEN-based specific transcript knock-down of PIWIL2 suppresses cell growth in HepG2 tumor cell

Y. Chen[1], W. Hu[1], Y. Lu, S. Jiang, C. Li, J. Chen, D. Tao, Y. Liu, Y. Yang and Y. Ma

Department of Medical Genetics, State Key Laboratory of Biotherapy, West China Hospital, Sichuan University, Chengdu, 610000, China

Received 27 March 2014; revision accepted 6 May 2014

Abstract

Objectives: PIWIL2 is widely expressed in various tumours and implicated in playing a role in tumourigenesis. For a more thorough study of PIWIL2 functions in tumour cells, we aimed to establish PIWIL2-specific transcript knock-down/knockout HepG2 cell lines using transcription activator-like effector nuclease (TALEN) technology. Furthermore, we proposed to use the cell models to explore PIWIL2 functions in TGF-β signalling in HepG2 cells. HepG2s are human hepatocellular carcinoma cells.

Materials and methods: We established PIWIL2 knock-down or knock-out cell lines in HepG2 using TALEN technology. Next, we sought to use the cell line models to investigate effects of full length PIWIL2-specific transcripts in cell proliferation induced by TGF-β.

Results: First, we established PIWIL2-specific transcript mono-allele and bi-allele knockout HepG2 cell lines. By using the cell line models, we found that specific transcript knockdown of full length PIWIL2 can suppress cell proliferation, while ectopic expression of PIWIL2 enhanced proliferation of HepG2 by suppressing the TGF-β pathway. Furthermore, we demonstrated that PIWIL2 can interact with HSP90 to prevent formation of HSP90–TβR complexes, which promote degradation of TβRs.

Conclusions: Taken together, our study revealed critical negative regulation of TGF-β signalling by PIWIL2 in HepG2 tumour cells, and provided an effective strategy to study specific gene transcript functions in cells.

Correspondence: Y. Ma, Department of Medical Genetics, State Key Laboratory of Biotherapy, West China Hospital, Sichuan University, Chengdu, China. Tel.: +86-028-85164010; Fax: +86-028-85164009; E-mail: mayongxin@gmail.com

[1]These authors contributed equally to this work.

Introduction

PIWI proteins contain two highly conserved domains (PIWI and PAZ domains), and have multiple biological functions in stem cell self-renewal, gametogenesis, embryogenesis and transposon control, in diverse organisms ranging from *Drosophila* to humans (1–6). In *Drosophila*, *piwi* is required in somatic cell signalling, to maintain germline stem cells, and to have a role as cell-autonomous promoter of germline stem cell division (2). *piwi* in zebrafish (*ziwi* and *zili*) has an effect on germ cell differentiation, early embryogenesis and transposon silencing (5,7,8). Three PIWI proteins are expressed in mice: MIWI, MILI and MIWI2, and their deficiency can cause incompleted spermatogenesis (9–11). Four members of the PIWI subfamily have been identified in the human genome (PIWIL1/Hiwi, PIWIL2/Hili, PIWIL3 and PIWIL4/Hiwi2). In normal tissues, PIWIL2 (located on chromosome 8q24), is mainly expressed in testis and in the embryo (12). Also, it has been reported that PIWIL2 and its variants PIWIL2-Like (PL2L) proteins exist widely in various types of human cancer and tumour cell lines, suggesting that they may play roles of oncogenic fate determinants. PL2L proteins so far reported include PL2L80, PL2L60, PL2L50 and PL2L40 (12–16).

The transcription activator-like effector nuclease (TALEN) system has been shown to be a new tool to generate gene knockout in zebrafish, rats and cell lines (17–19). Due to a double recognition target site, TALEN technology is highly specific to the target gene. TALENs are fusion proteins which contain a DNA-binding domain and a *Fok* I endonuclease domain. The two TALENs bind to their target sites in a genome at an appropriate distance. Then, two *Fok* I components dimerize and cause double-strand breaks, resulting in stimulation of breakage repair mechanisms in cell nuclei (17,20). Breakage is repaired by non-homologous end-joining (NHEJ), which frequently generates small insertions or deletions. Here, we screened frameshift mutant as the HepG2 PIWIL2 knockout cell model to investigate PIWIL2 functions in TGF-β signalling.

TGF-β signalling is highly controlled in normal cells, and has been found to play diverse roles in regulating growth, differentiation and immune response as well as development in multi-organ systems (21–26). Active TGF-β initiates signalling by binding to type I (TβRI) and type II (TβRII) receptors. TβRI is phosphorylated by TβRII, then it phosphorylates and activates members of the Smad family of tumour suppressors (termed R-Smads), including Smad2 and Smad3 (27). TGF-β induces inhibition of proliferation in many cell types, by repressing expression of oncogenes and inducing expression of cyclin-dependent kinase inhibitor p21 (28–31). TGF-β signalling acts as a paracrine suppressor on proliferation of hepatocytes in normal liver tissue (32). Also, in hepatocellular carcinoma (HCC) cells, TGF-β can induce senescence and tumour growth inhibition, and these effects are relevant to expression of p21 and p15 (33). A recent study also shown that attenuation of TGF-β signalling appears to be needed for development of HCC, but also there is requirement for TGF-β signalling, for survival and malignancy (34).

We have previously reported that PIWIL2 can regulate TGF-β signalling in HEK293 cells (35). Thus, we next explored whether expression of PIWIL2 in HepG2 tumour cells would be able to promote cell proliferation by attenuating TGF-β signalling. Early research has also shown that PIWIL2 and PL2L proteins exist in tumour cells and that they may have different functions (14). Here we used TALEN technology to establish PIWIL2-specific transcript mono-allele and bi-allelic knockout HepG2 cell lines in which we could explore the functions of PIWIL2 rather than PL2L proteins. By using these cell models and PIWIL2 ectopic expressed HepG2 cells, we demonstrated that PIWIL2 promoted degradation of TβRs and attenuated TGF-β signalling. It then lead to suppression of TGF-β-induced growth inhibition, revealing critical negative regulation of TGF-β signalling by PIWIL2 in these tumour cells.

Materials and methods

Expression vectors, shRNA and antibodies

PIWIL2, HSP90 and ubiquitin expression vectors are maintained in our laboratory as previously described (35). shPIWIL2 is PIWIL2 siRNA expression vector, and RNA interference sequence (5′ ACC GGC CTG GGT TGA ACT AAA 3′) was cloned into pGPU6/GFP/Neo plasmid (GenePharma, Shanghai, China). Rabbit anti-PIWIL2 antibody was obtained from Santa Cruz Biotechnology (USA) as were goat anti-HSP90 antibody and rabbit anti-Smad4 antibody. Rabbit anti-p21 antibody, rabbit anti-phospho-Smad3 antibody, rabbit anti-Smad2 antibody, rabbit anti-Smad3 antibody and rabbit anti-GAPDH antibody were purchased from Epitomics (USA). Rabbit anti-phospho-Smad2 antibody, rabbit anti-TβRI antibody, rabbit anti-TβRII antibody and mouse anti-HA antibody were obtained from Cell Signaling Technology (USA). Mouse anti-Myc antibody was purchased from Zhongshan Goldenbridge (Beijing, China).

Cell culture, transfection and treatment

HepG2 cells are permanently maintained in our laboratory. Here, they were cultured in DMEM/10% FBS and transfected by using jetPRIME (PloyPlus, France) according to the manufacturers' protocols. Forty eight hours after transfection, cell treatments were carried out in reduced-serum media (0.2% FBS), and TGF-β (Peprotech, USA) was added as indicated, to final concentration of 10 ng/ml. Where specified, cells were treated with proteasome inhibitor MG132 (Zhongshan Goldenbridge) at final concentration of 20 μM. Cells were harvested and analysed by western blotting using appropriate antibodies. All following experiments were repeated at least three times unless stated otherwise.

Knockout of PIWIL2 using TALEN technology

PIWIL2 knockout cell lines were acquired by transcription activator-like effector nuclease (TALEN) technology. TALEN plasmids were purchased from ViewSolid Biotech (Beijing, China). Target sequences of TALENs are as follows: GCC AGG CTG TAC GGA T and CCA AAG GTT TAG AAG CT for *PIWIL2* gene exon2, which is located on chromosome 8p24. Between the two binding sites is an 18 bp spacer with *Msc* I sequence (GCC AGG CTG TTG GCC ACA, *Msc* I underlined) for enzyme digestion identification. To obtain PIWIL2 knockout cells, the pair of TALEN plasmids was co-transfected to HepG2 cells at molar ratio of 1:1, using 6-well plates. After 72 h culture, cells were digested with trypsin and counted. Then, they were subcultured into 96-well plates and subjected to single cell cloning. After individual cell clones expanded, genomic DNA was extracted from the clones using TransDirect™ Animal Tissue PCR Kit (TransGen Biotech, Beijing, China). Genomic DNA extracted from these monoclonal HepG2 cells was amplified by PCR (Forward primer, 5′ GAG GGA TTG TTA ATG AAG GAT GTT T 3′; Reverse primer, 5′ ACT TTG AAA TCC ATT ACT TCC TCT G 3′). PCR products were digested by endonuclease *Msc* I (Thermo Scientic, USA) for identification. Then, identified PCR products containing mutated sites were cloned into pMD19-T vector (Takara, Japan) and sequenced, to identify whether the mutation was frameshift mutation.

Single strand conformation polymorphism assay (SSCP)

We used single strand conformation polymorphism (SSCP) analysis to screen *PIWIL2* bi-allele mutant monoclonal cell lines. As DNA fragments for SSCP analysis would be 200–300 bp, primers were designed for PCR (Forward primer, 5′ CTT TCC GAC CAT CGT TCA 3′; Reverse primer, 5′ CTC TGG CTT TCC AAA TAC AT 3′). Monoclonal cells were collected and genomic DNA was extracted for PCR amplification. PCR products were mixed with equal volumes of 2 × SSCP loading buffer (95% formamida, 20 mM EDTA, 0.05% xylene cyanol, 0.05% bromophenol blue, pH 8.0), heated to 96 °C for 10 min, then rapidly cooled on ice for 5 min. Products were then separated by electrophoresis with 15% non-denaturing polyacrylamide gel, and detected by silver staining. In detail, gels were fixed in 7.5% acetic acid for 30 min after electrophoresis, washed three times in ddH_2O for 2 min, then washed in 15% formaldehyde for 5 min, followed by immersion in silver nitrate solution for 20 min. Gels were developed by merging with 3% Na_2CO_3 solution pre-cooled to 4 °C. Finally the reaction was stopped with 7.5% acetic acid.

Co-immunoprecipitation and western blotting

Cells were lysed in universal protein extraction buffer (BioTeke, Beijing, China) applied with protease inhibitor cocktail (Roche, Switzerland) 48 h after transfection. For co-immunoprecipitation, extracted proteins were immunoprecipitated with 1 μg antibody and 30 μl protein A+G agarose beads (Beyotime, Shanghai, China), then precipitated by centrifugation at 1000 ***g*** for 5 min. Complexes were washed four times in ice-cold PBS Buffer (pH 7.4). For western blotting, proteins were mixed with 5 × SDS loading buffer (BioTeke) and heated to 95 °C for 8 min before separating with 4–12% SDS-PAGE. Proteins were then transferred to polyvinylidene difluoride membranes (Millipore, Massachusetts, USA), and detected with appropriate primary antibodies and horseradish peroxidase-conjugated secondary antibodies. Finally, membranes were visualized using chemiluminescent HRP substrate (Millipore).

Immunofluorescence

Cells were fixed for 15 min in 4% formaldehyde in PBS, permeabilized for 10 min with 0.5% Triton X-100, blocked in 1% BSA for 30 min, incubated with relevant primary antibody overnight at 4 °C and finally incubated with FITC-labelled, or Cy3-labelled secondary antibody (Beyotime) for 2 h at room temperature. Each step was followed by two 5 min washes in PBS. Prepared specimens were counterstained with 5 mg/ml DAPI for 2 min and observed using a fluorescence microscope (Olympus, Japan).

Cell viability assay

Cell viability was determined using a cell counting kit-8 (CCK-8, Beyotime) based on WST-8. WST-8 existing in CCK-8 solution reacts with mitochondrial dehydrogenase, and results in orange formazan deposition. A linear relationship between cell number and shade was used to evaluate cell proliferation. Briefly, HepG2 cells (2×10^3) were seeded in 96-well plates in DMEM (100 μl) containing 10% foetal bovine serum, and cultured overnight. After advisable plasmid transfection for 4 h, medium was renewed with fresh medium and TGF-β either added or not added, and continuously cultured for 72 h. CCK-8 solution (10 μl) was added to each of the 96-well plates, and cultures were incubated for 90 min at 37 °C. Absorbance at 450 nm was measured using an automatic microplate reader (BioTeke, Beijing, China). A standard curve was be set up to deduce cell number .Experiments were performed in sextuplicate and repeated three times. Results were further analysed using Origin 8.0 software.

Results

Establishment of PIWIL2 mono-allelic knockout cell lines

First, we examined whether the TALEN system was useful on the HepG2 cell genome. To test this, the pair of TALEN plasmids were co-transfected to HepG2 cells over a concentration gradient. To evaluate efficiencies of genome editing, nucleotide sequences of TALEN cleavage sites were identified by PCR amplification based on genomic DNA extracted from TALEN-transfected cells. Then PCR products were digested by *Msc* I and agarose gel electrophoresis was performed (Fig. 1b).

PCR products amplified from TALEN-transfected cells had incomplete digestion (annotated as Edited DNA) compared to controls. Results showed that plasmids could, indeed, be useful for knocking out *PIWIL2* in HepG2 cells. Genome editing activities were confirmed at a level in the order of 10%, through gray analysis (data not shown).

To establish stable knockout cell lines, TALEN-transfected cells were subcultured in 96-well plates to obtain a monoclonal cell line. Then, expanded monoclonal cells were identified by *Msc* I digestion (Fig. 1c). By screening and sequencing, we obtained three mutant cell lines (Fig. 2a). For further identification, the TALEN pair-targeted region was amplified by PCR and subjected to

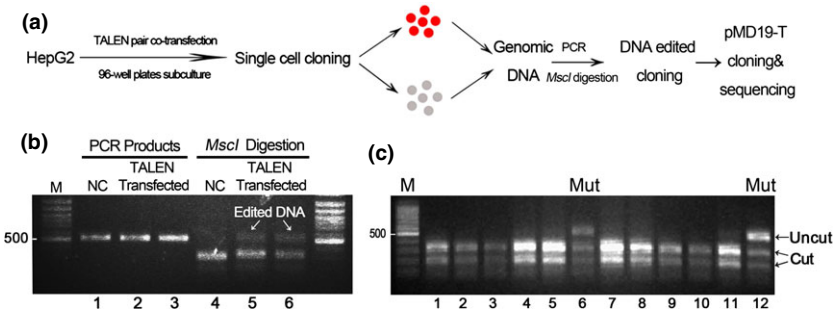

Figure 1. Effects of TALEN on HepG2 genomic DNA. (a) Schematic diagram of the screening experiment. HepG2 cells were transfected with the pair of TALEN plasmids. Seventy two hours later, cells were subjected to single cell cloning in 96-well plates. After individual cell clones expanded, genomic DNA was extracted from these cells. The TALEN pair target region was amplified by PCR and subjected to pMD19-T cloning and sequencing. (b) The HepG2 cell genome was edited by the pair of TALEN plasmids. Cells were transfected with TALEN plasmids (lane 2 and 4: 1 μg, lane 3 and 6: 2 μg), and cultured for 72 h before DNA was extracted for PCR, then *Msc* I digestion. NC represents negative controls with no transfection. (c) Screen mutants by *Msc* I digestion analysis of TALEN target region. Lanes 6 and 12 show partial digestion, regarded as mutants (annotated as Mut) for further testing.

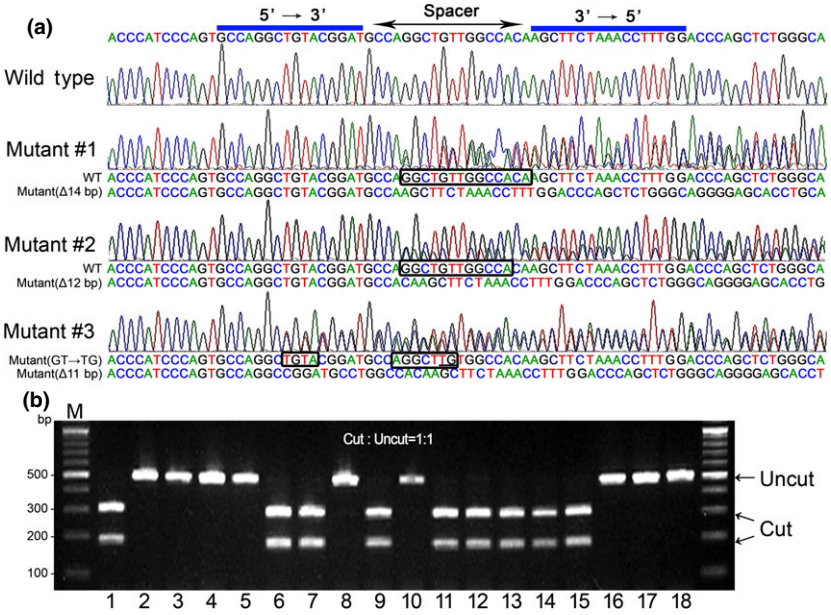

Figure 2. Screen and analysis of *PIWIL2* mono-allelic mutations. (a) Sequencing and alignment of mutations. PCR products amplified from wild type and mutants genomic DNA were sequenced. The TALEN pair target sequences were coloured in blue. The deleted sequences of allele were indicated with black box on the other allele. The sizes of deletions were shown with △. An unexpected mutation (GT → TG) in clone Mutant #3 was observed and underlined. (b) An allele analysis of clone Mutant #1. The PCR products were cloned into pMD19-T vector. Eighteen positive clones were analysed by PCR amplification and *Msc* I digestion.

pMD19-T cloning and sequencing. As shown in Fig. 2b, pMD19-T vectors labouring PCR products of clone Mutant #1 (In Fig. 2a) were analysed by PCR and *Msc* I digestion. Then they were sequenced to identify allelic mutants (data not shown). Finally, we detected two mono-allele frameshift mutant cell lines. We used the 14 bp deleted result for further testing.

Abnormal chromosome numbers (aneuploidy) and structural chromosomal aberrations are invariably found in tumour cells, and this may induce abnormal states of gene copies. We were informed by websites (http://www.dsmz.de and http://hepg2.com) that HepG2 cells do not usually have numerical abnormality on chromosome 8 where *PIWIL2* is located. Also, analysis of *Msc* I digestion showed that the mutant DNA band accounted for around 50% of our obtained *PIWIL2* mono-allelic mutant cells.

Establishment of PIWIL2 bi-allelic knockout cell lines

Based on the *PIWIL2* mono-allelic knockout cell lines, we continued to generate bi-allelic knockout cells. We used single strand conformation polymorphism analysis (SSCP) to screen the bi-allelic mutants (Fig. 3a). Compared to *Msc* I digestion, this method can reveal the mutation with no change at the *Msc* I site. Similarly, genomic DNA of mutants identified by SSCP was amplified by PCR and subjected to pMD19-T cloning

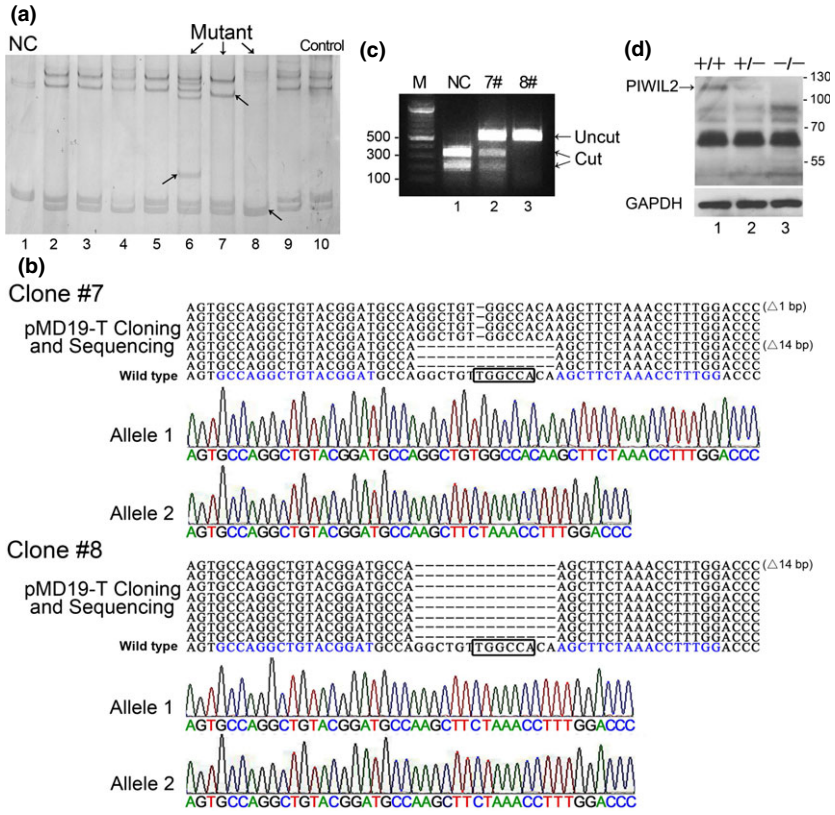

Figure 3. Identification of *PIWIL2* bi-allelic knockout cell lines. (a) Single strand conformation polymorphism (SSCP) analysis to screen monoclonal bi-allele mutant cell lines. NC represents normal HepG2 cells. Control represents 14 bp deleted *PIWIL2* mono-allelic knockout cell line. Compared to controls, lanes 6, 7 and 8 indicated second mutation. Remarkable differences with controls – marked with arrows. (b) Identification of *PIWIL2* bi-allelic knockout cell lines. Mutants in (a) were further identified by pMD19-T cloning and sequencing to analyse allelic mutations. Clones #7 and #8 respectively represent cell lines chosen as mutants in lanes 7 and 8 in (a). Other mutants did not have frameshift mutations on one allele (data not shown). Nucleotide sequences of mutated alleles – indicated with dashes. (c)Further identification with PCR amplification and restriction endonuclease analysis of the two cell clones in (b). NC represents normal HepG2 cells. (d) Western bolt analysis of expression of PIWIL2 in normal HepG2, *PIWIL2*+/− and *PIWIL2*−/− cells.

and sequencing. Sequence alignment results showed that we obtained two *PIWIL2* bi-allelic knockout cell lines (Fig. 3b). Clone #7 showed a renewed *Msc* I site on one allele, and #8 showed *Msc* I site losing both alleles. They both have second frameshift mutations, one having a 1 bp deletion and the other a 14 bp deletion. Further identification for PCR amplification and restriction endonuclease analysis was in accordance with the sequencing results (Fig. 3c). Compared to controls, TALEN targeted region of clone #7 had partial digestion by *Msc* I, while the region of clone #8 could not be cut.

Further, western blot analysis showed that the 110KD band was reduced or undetectable, indicating that the full length transcript encoding intact PIWIL2 protein was mono-allelic (*PIWIL2*+/−) or bi-allelic knocked out (*PIWIL2*−/−) (Fig. 3d). In these knockout cells, we did not find any reduction of PL2L proteins. Interestingly, we observed that PL2L80 level was upregulated in *PIWIL2*−/− cells, while not notably alternated in *PIWIL2*+/− cells.

PIWIL2 suppressed cell population growth by inhibiting TGF-β signalling in HepG2 cells

After obtaining *PIWIL2*+/− and *PIWIL2*−/− cell lines using the TALEN system, we tested cell proliferation levels. Normal HepG2, *PIWIL2*+/− and *PIWIL2*−/−

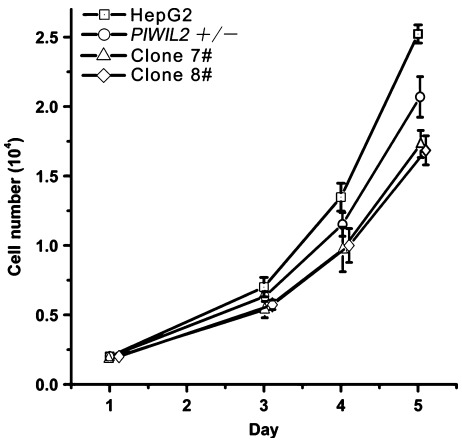

Figure 4. Loss of PIWIL2 reduced HepG2 cell proliferation. Cell proliferation levels of normal HepG2, *PIWIL2*+/− and *PIWIL2*−/− cell lines. Clone #7 and clone #8 represent the two PIWIL2 knockout cell lines mentioned earlier. Respectively at days 3, 4 and 5, we used CCK-8 assay to evaluate cell proliferation levels.

cells of equal number were respectively seeded into 96-well plates. Respectively after 3, 4 and 5 days, we used CCK-8 assay to evaluate cell proliferation levels. Results showed that loss of PIWIL2 reduced HepG2 cell proliferation (Fig. 4). Previous study indicated that TGF-β signalling induced senescence and inhibited

tumour growth in HCCs (33). Thus, we next explored association between PIWIL2 and TGF-β signalling in HepG2 cell population growth.

As mentioned above, the *PIWIL2*+/− cells had lower levels of 110kD protein encoded by the full-length PIWIL2 transcript, while PL2L proteins were not obviously altered. In *PIWIL2*−/− cells, we observed that the PL2L80 was upregulated. For simplicity, we chose the *PIWIL2*+/− cells model to explore effects of PIWIL2 rather than PL2L variants in TGF-β signalling. The Smad pathway is downstream of TGF-β receptors, which can induce upregulation of cell cycle inhibitor p21 (36,37). Initially, normal HepG2 cells and *PIWIL2*+/− cells were treated by TGF-β stimulation. We then checked the effects on the TGF-β pathway induced by PIWIL2 deficiency. Western blot analysis showed that loss of PIWIL2 promoted phosphorylation of Smad2/3, while levels of p21 induced by TGF-β were also prominently upregulated; also, amounts of Smad2/3/4 total protein levels were not notably altered. These occurred in cells treated or not treated with exogenous TGF-β stimulation. We also detected TβRI and TβRII levels to confirm whether PIWIL2 attenuated TGF-β signalling at TGF-β receptor protein level. Results showed that TβR levels increased when PIWIL2 was knocked down (Fig. 5a). These findings indicated that PIWIL2 downregulated TGF-β receptors and inhibited TGF-β signalling.

To further confirm that PIWIL2 plays a role in attenuating Smad2/3 phosphorylation and p21 expression, we overexpressed PIWIL2 by transfecting PIWIL2 expression vector over a concentration gradient, and analysed effects on expression of p21 and activation of Smad2/3 induced by TGF-β. Overexpression of PIWIL2 reduced expression of p21, TβRI, TβRII and phosphorylation of Smad2/3 induced by TGF-β, while expression of Smad2/3 was not notably altered. (Fig. 5b). All above results suggested that PIWIL2 reduced TGF-β signalling at the level of TβRs and attenuated downstream events, in a dose-dependent manner.

Finally, we detected effects of PIWIL2 on HepG2 cell proliferation meditated by TGF-β. CCK-8 assay showed that ectopic expression of PIWIL2 positively regulated proliferation of HepG2 cells (Fig. 5c). In pcDNA3.1- or shPIWIL2-transfected cells, treatment with TGF-β induced obvious proliferation inhibition compared to untreated cells. However, when overexpressed PIWIL2, TGF-β-induced proliferation inhibition was attenuated, and there was no significant difference between proliferation levels in cells treated or not treated with TGF-β (Fig. 5d). These results suggest that existence of PIWIL2 promoted tumour cell proliferation by weakening proliferation inhibition of TGF-β signalling.

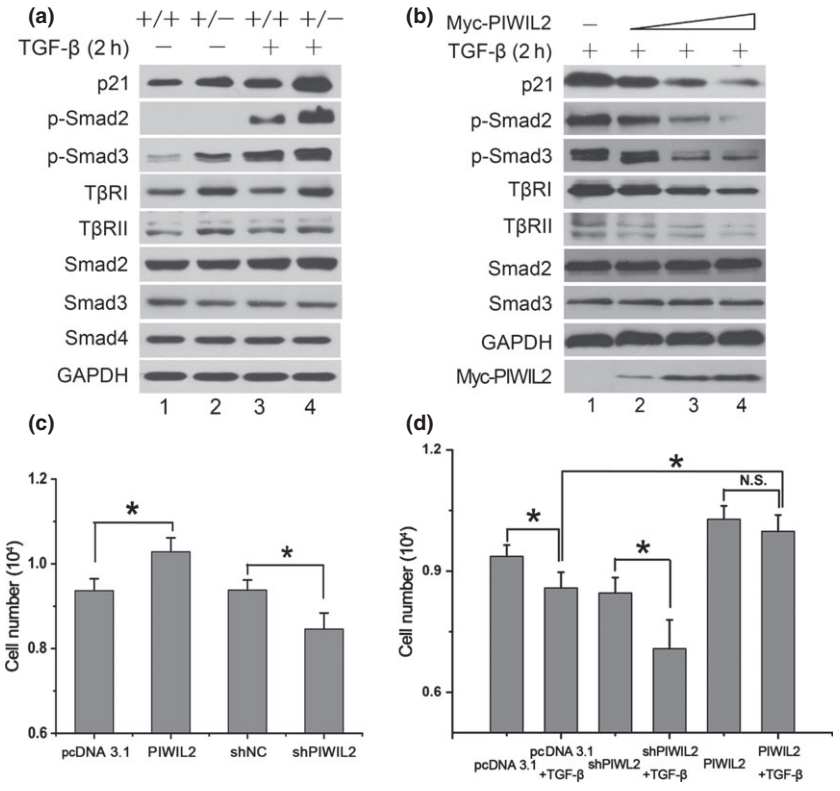

Figure 5. PIWIL2 promoted cell population growth by inhibiting TGF-β signalling in HepG2 cells. (a) Knockdown of PIWIL2 upregulated p21, TβRI, TβRII and phosphorylated Smad2/3 with or without TGF-β stimulation. Normal HepG2 and *PIWIL2*+/− cells were treated or not treated with TGF-β for 2 h before harvesting. (b) Ectopic expression of PIWIL2 reduced level of p21, TβRI, TβRII and prevented Smad2/3 activation. HepG2 cells were transfected with PIWIL2 over a concentration gradient and treated with TGF-β before cells were harvested. (c) and (d) PIWIL2 attenuated TGF-β-induced population growth inhibition. HepG2 cells were respectively transfected with pcDNA3.1, PIWIL2, shControl and shPIWIL2, and cultured in complete medium with or without TGF-β stimulation for 96 h before cells were analysed with CCK-8. Each experiment was performed in triplicate. *Indicates $P < 0.05$. N.S. indicates $P > 0.05$.

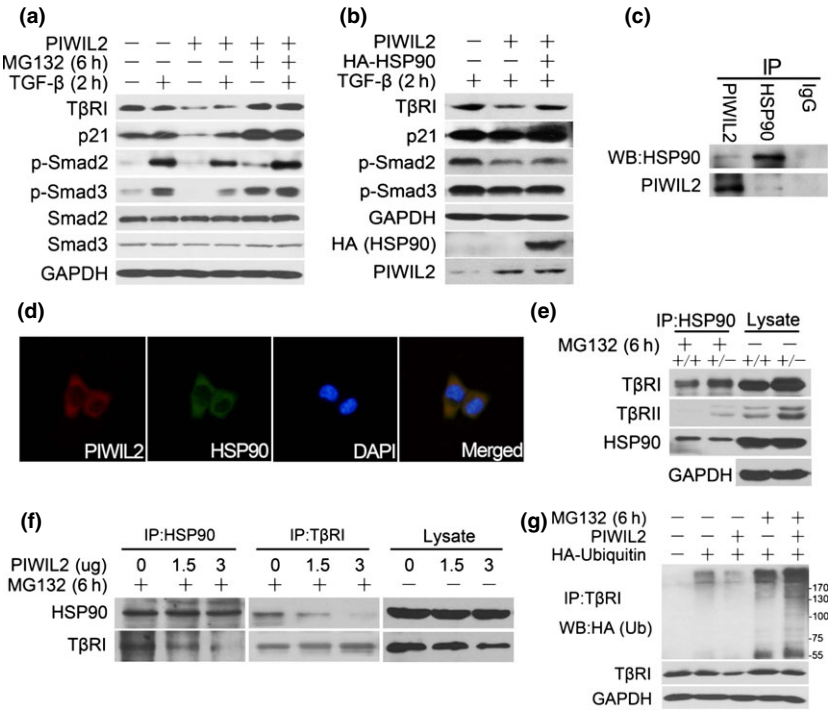

Figure 6. PIWIL2 regulated degradation of TβRs *via* HSP90. (a) PIWIL2 promoted TβR degradation. HepG2 cells were transfected with Myc-PIWIL2, treated with MG132 for 6 h, and TGF-β for the last 2 h. (b) Reduction of TβRs and downstream events mediated by PIWIL2 was rescued by overexpression of HSP90. (c) Endogenous interactions between PIWIL2 and HSP90 in HepG2 cells. Co-IP was performed with anti- PIWIL2 or anti-HSP90, followed by western blotting. (d) Both PIWIL2 and HSP90 were co-localized mainly in cytoplasm. HepG2 cells were transfected with Myc-PIWIL2 and harvested for immunofluorescence with anti-Myc and anti-HSP90 antibodies. (e) PIWIL2 reduced interaction of HSP90 and TβRs. Normal and PIWIL2 knockdown cells were treated with MG132 before harvesting, and lysates were subjected to immunoprecipitation with anti-HSP90 antibody. (f) PIWIL2 attenuates interaction of HSP90 and TβRs. HepG2 cells were transfected with Myc-PIWIL2 over a concentration gradient. Forty eight hours later, cells were treated with MG132 before harvesting, and lysates were subjected to immunoprecipitation or western blot analysis. (g) PIWIL2 improved TβRI ubiquitination. HepG2 cells were co-transfected with Myc-PIWIL2 and HA-ubiquitin, then treated with MG132 and stimulated with TGF-β before harvesting. HA-ubiquitin was precipitated with anti-HA antibody, then ubiquitination and degradation of TβRI were determined by immunoblotting with anti-TβRI antibody.

PIWIL2 promoted degradation of TβRs

We detected the effect on TβR stability induced by PIWIL2. Cells were treated with proteasome inhibitor MG132 for 6 h, and TGF-β was added for the last 2 h. In PIWIL2 overexpressing cells, TβRI levels were reduced by PIWIL2, paralleling loss of phosphorylated Smad2/3, while Smad2/3 protein levels remained stable. These alterations were reversed by MG132 treatment, to some extent (Fig. 6a), suggesting that PIWIL2 attenuated stability of TβR proteins, promoted degradation of TβRI, and blocked Smad2/3 phosphorylation, thus causing inhibition of TGF-β signalling.

PIWIL2 regulated degradation of TβRs via HSP90

HSP90, the 90-kDa heat-shock protein, is an abundant molecular chaperone which can stabilize TβRs and prevent ubiquitination and degradation of TβRs(38). We have also previously reported HSP90 to be a critical factor involved in regulation of TGF-β signalling, induced by PIWIL2 in HEK293 cells (35). Thus, we explored whether a similar mechanism existed in HepG2 tumour cells. Western blotting results revealed that in cells co-transfected with HSP90 and PIWIL2, TβR reduction and downstream events mediated by PIWIL2 could be rescued (Fig. 6b). Then we examined whether PIWIL2 would interact with HSP90 in tumour cells. To confirm the physical interaction between PIWIL2 and HSP90, we carried out reciprocal immunoprecipitation of endogenous PIWIL2 and HSP90 in HepG2s (Fig. 6c). Co-immunoprecipitation experiments revealed that PIWIL2 bound to HSP90. Also, immunofluorescence experiments showed that PIWIL2 was located mostly in the cytoplasm, and overlapped with HSP90 (Fig. 6d). These data indicate that PIWIL2 can interact with HSP90 in HepG2 cells.

Following this, we detected the effect of PIWIL2 on binding ability of HSP90 and TβR. When PIWIL2 was knocked out, co-immunoprecipitation experiments showed that HSP90 had stronger combining capacity with

TβRs (Fig. 6e). Furthermore, endogenous TβRI was immunoprecipitated by HSP90 from PIWIL2 overexpressing HepG2 cell lysates over a concentration gradient, using TβRI antibody. PIWIL2 overexpression reduced combining capacity of HSP90 with TβRI (Fig. 6f).

Finally, we tested whether PIWIL2 would promote TβR ubiquitination. HepG2 cells were transfected with Myc-PIWIL2 and HA-ubiquitin. Endogenous TβRI was co-immunoprecipitated with HA-tag ubiqutin and ubiquitination of TβRI was detected by TβRI antibody. Less ubiquitination of TβRI was detected in PIWIL2 overexpressing HepG2 cells compared to controls. When supplied with MG132, ubiquitination of TβRI was significantly higher in PIWIL2 overexpressing cells in contrast to controls (Fig. 6g). These studies implied that PIWIL2 competed with TβRs for HSP90, to weaken TβR stability, promote its degradation, and finally to negatively regulate TGF-β signalling in HepG2 tumour cells.

Discussion

PIWIL2 has been widely reported to exist in a variety of tumour cells (13,15,16). Recent research has also shown that *PIWIL2* variants exist in tumour cells and express PL2L proteins, which may have different functions from full-length PIWIL2 (14). Thus it has been necessary to explore mechanisms of PIWIL2 and its variants, in tumourigenesis. In our study, we first used TALEN technology to establish PIWIL2 mono-allelic and bi-allelic knockout cell line models. Protein expression analysis showed reduction in undetected full length PIWIL2. Interestingly, we also found that with totally absent PIWIL2, upregulation of PL2L80 was detected, while not notably alternated in *PIWIL2*+/− cells (Fig. 4d). Thus, for simplicity, *PIWIL2*+/− cells were chosen as the cell model to explore effects of PIWIL2 in TGF-β signalling.

The present study in cell models revealed that existence of PIWIL2 maintained HepG2 cell proliferation (Fig. 4). Recent studies showed that TGF-β stimulation induced senescence and inhibited tumour growth in HCCs (33,34). We have previously reported that PIWIL2 regulated TGF-β signalling in HEK293 cells (35). So next we explored whether cell proliferation inhibition induced by PIWIL2 loss was related to TGF-β signalling. Also, it has been reported that many components of TGF-β signalling (such as TGF-β type I and type II receptors) can be inactivated by different mechanisms in human tumour cells (39,40). Here our study showed that *PIWIL2* promoted degradation of TβRs and suppressed TGF-β signalling.

By using the established specific transcript knockdown of PIWIL2 cell line models and performing transfection in HepG2 cells, we have been able to present several pieces of evidence demonstrating that PIWIL2 blocks formation of HSP90–TβR complexes, weakens stability of TβR and finally promotes tumour cell proliferation. Our present study reveals critical negative regulation of TGF-β signalling by PIWIL2 in these tumour cells, and provides a more comprehensive insight into roles of PIWIL2. In addition, PIWIL2 mono-allelic and bi-allelic knockout provides a novel strategy to investigate functions of a gene, its proteins and variants in cells.

Acknowledgements

This study was supported by the National Basic Research Program of China (973 Program, 2012CB947600), National Natural Science Foundation of China (31070676, 90919006 and 31300961).

References

1 Aravin AA, Hannon GJ, Brennecke J (2007) The Piwi-piRNA pathway provides an adaptive defense in the transposon arms race. *Science* **318**, 761–764.
2 Cox DN, Chao A, Baker J, Chang L, Qiao D, Lin H (1998) A novel class of evolutionarily conserved genes defined by piwi are essential for stem cell self-renewal. *Genes Dev.* **12**, 3715–3727.
3 Carmell MA, Xuan Z, Zhang MQ, Hannon GJ (2002) The Argonaute family: tentacles that reach into RNAi, developmental control, stem cell maintenance, and tumorigenesis. *Genes Dev.* **16**, 2733–2742.
4 Seipel K, Yanze N, Schmid V (2004) The germ line and somatic stem cell gene Cniwi in the jellyfish Podocoryne carnea. *Int. J. Dev. Biol.* **48**, 1–7.
5 Sun H, Li D, Chen S, Liu Y, Liao X, Deng W, *et al.* (2010) Zili inhibits transforming growth factor-beta signaling by interacting with Smad4. *J. Biol. Chem.* **285**, 4243–4250.
6 Yin H, Lin H (2007) An epigenetic activation role of Piwi and a Piwi-associated piRNA in Drosophila melanogaster. *Nature* **450**, 304–308.
7 Houwing S, Kamminga LM, Berezikov E, Cronembold D, Girard A, van den Elst H, *et al.* (2007) A role for Piwi and piRNAs in germ cell maintenance and transposon silencing in Zebrafish. *Cell* **129**, 69–82.
8 Houwing S, Berezikov E, Ketting RF (2008) Zili is required for germ cell differentiation and meiosis in zebrafish. *EMBO J.* **27**, 2702–2711.
9 Deng W, Lin H (2002) miwi, a murine homolog of piwi, encodes a cytoplasmic protein essential for spermatogenesis. *Dev. Cell* **2**, 819–830.
10 Carmell MA, Girard A, van deKant HJ, Bourc'his D, Bestor TH, de Rooij DG, *et al.* (2007) MIWI2 is essential for spermatogenesis and repression of transposons in the mouse male germline. *Dev. Cell* **12**, 503–514.
11 Kuramochi-Miyagawa S, Kimura T, Ijiri TW, Isobe T, Asada N, Fujita Y, *et al.* (2004) Mili, a mammalian member of piwi family gene, is essential for spermatogenesis. *Development* **131**, 839–849.
12 Sasaki T, Shiohama A, Minoshima S, Shimizu N (2003) Identification of eight members of the Argonaute family in the human genome small star, filled. *Genomics* **82**, 323–330.
13 Lee JH, Schutte D, Wulf G, Fuzesi L, Radzun HJ, Schweyer S, *et al.* (2006) Stem-cell protein Piwil2 is widely expressed in

tumors and inhibits apoptosis through activation of Stat3/Bcl-XL pathway. *Hum. Mol. Genet.* **15**, 201–211.
14 Ye Y, Yin DT, Chen L, Zhou Q, Shen R, He G, *et al.* (2010) Identification of Piwil2-like (PL2L) proteins that promote tumorigenesis. *PLoS ONE* **5**, e13406.
15 Liu JJ, Shen R, Chen L, Ye Y, He G, Hua K, *et al.* (2010) Piwil2 is expressed in various stages of breast cancers and has the potential to be used as a novel biomarker. *Int. J. Clin. Exp. Pathol.* **3**, 328–337.
16 He G, Chen L, Ye Y, Xiao Y, Hua K, Jarjoura D, *et al.* (2010) Piwil2 expressed in various stages of cervical neoplasia is a potential complementary marker for p16. *Am. J. Transl. Res.* **2**, 156–169.
17 Bedell VM, Wang Y, Campbell JM, Poshusta TL, Starker CG, Krug RG 2nd, *et al.* (2012) In vivo genome editing using a high-efficiency TALEN system. *Nature* **491**, 114–118.
18 Sung YH, Baek IJ, Kim DH, Jeon J, Lee J, Lee K, *et al.* (2013) Knockout mice created by TALEN-mediated gene targeting. *Nat. Biotechnol.* **31**, 23–24.
19 Hu R, Wallace J, Dahlem TJ, Grunwald DJ, O'Connell RM (2013) Targeting human microRNA genes using engineered Tal-effector nucleases (TALENs). *PLoS ONE* **8**, e63074.
20 Miller JC, Tan S, Qiao G, Barlow KA, Wang J, Xia DF, *et al.* (2011) A TALE nuclease architecture for efficient genome editing. *Nat. Biotechnol.* **29**, 143–148.
21 Massague J, Blain SW, Lo RS (2000) TGFbeta signaling in growth control, cancer, and heritable disorders. *Cell* **103**, 295–309.
22 Heldin CH, Landstrom M, Moustakas A (2009) Mechanism of TGF-beta signaling to growth arrest, apoptosis, and epithelial-mesenchymal transition. *Curr. Opin. Cell Biol.* **21**, 166–176.
23 Moustakas A, Pardali K, Gaal A, Heldin CH (2002) Mechanisms of TGF-beta signaling in regulation of cell growth and differentiation. *Immunol. Lett.* **82**, 85–91.
24 ten Dijke P, Arthur HM (2007) Extracellular control of TGFbeta signalling in vascular development and disease. *Nat. Rev. Mol. Cell Biol.* **8**, 857–869.
25 Siegel PM, Massague J (2003) Cytostatic and apoptotic actions of TGF-beta in homeostasis and cancer. *Nat. Rev. Cancer* **3**, 807–821.
26 de Caestecker M (2004) The transforming growth factor-beta superfamily of receptors. *Cytokine Growth Factor Rev.* **15**, 1–11.
27 Moustakas A, Souchelnytskyi S, Heldin CH (2001) Smad regulation in TGF-beta signal transduction. *J. Cell Sci.* **114**, 4359–4369.
28 Massague J (2004) G1 cell-cycle control and cancer. *Nature* **432**, 298–306.
29 Laiho M, DeCaprio JA, Ludlow JW, Livingston DM, Massague J (1990) Growth inhibition by TGF-beta linked to suppression of retinoblastoma protein phosphorylation. *Cell* **62**, 175–185.
30 Feng XH, Liang YY, Liang M, Zhai W, Lin X (2002) Direct interaction of c-Myc with Smad2 and Smad3 to inhibit TGF-beta-mediated induction of the CDK inhibitor p15(Ink4B). *Mol. Cell* **9**, 133–143.
31 Chen CR, Kang Y, Massague J (2001) Defective repression of c-myc in breast cancer cells: a loss at the core of the transforming growth factor beta growth arrest program. *Proc. Natl. Acad. Sci. USA* **98**, 992–999.
32 Bissell DM, Wang SS, Jarnagin WR, Roll FJ (1995) Cell-specific expression of transforming growth factor-beta in rat liver. Evidence for autocrine regulation of hepatocyte proliferation. *J. Clin. Invest.* **96**, 447–455.
33 Senturk S, Mumcuoglu M, Gursoy-Yuzugullu O, Cingoz B, Akcali KC, Ozturk M (2010) Transforming growth factor-beta induces senescence in hepatocellular carcinoma cells and inhibits tumor growth. *Hepatology* **52**, 966–974.
34 Mu X, Lin S, Yang J, Chen C, Chen Y, Herzig MC, *et al.* (2013) TGF-beta signaling is often attenuated during Hepatotumorigenesis, but is retained for the malignancy of hepatocellular carcinoma cells. *PLoS ONE* **8**, e63436.
35 Zhang K, Lu Y, Yang P, Li C, Sun H, Tao D, *et al.* (2012) HILI inhibits TGF-beta signaling by interacting with Hsp90 and promoting TbetaR degradation. *PLoS ONE* **7**, e41973.
36 Pardali K, Kurisaki A, Moren A, ten Dijke P, Kardassis D, Moustakas A (2000) Role of Smad proteins and transcription factor Sp1 in p21(Waf1/Cip1) regulation by transforming growth factor-beta. *J. Biol. Chem.* **275**, 29244–29256.
37 Moustakas A, Kardassis D (1998) Regulation of the human p21/WAF1/Cip1 promoter in hepatic cells by functional interactions between Sp1 and Smad family members. *Proc. Natl. Acad. Sci. USA* **95**, 6733–6738.
38 Wrighton KH, Lin X, Feng XH (2008) Critical regulation of TGFbeta signaling by Hsp90. *Proc. Natl. Acad. Sci. USA* **105**, 9244–9249.
39 Levy L, Hill CS (2006) Alterations in components of the TGF-beta superfamily signaling pathways in human cancer. *Cytokine Growth Factor Rev.* **17**, 41–58.
40 Kim SJ, Im YH, Markowitz SD, Bang YJ (2000) Molecular mechanisms of inactivation of TGF-beta receptors during carcinogenesis. *Cytokine Growth Factor Rev.* **11**, 159–168.